Tanaka, Hiroshi

Article

Theoretical analysis of solar thermal collector and flat plate bottom reflector with a gap between them

Energy Reports

Provided in Cooperation with:
Elsevier

Suggested Citation: Tanaka, Hiroshi (2015) : Theoretical analysis of solar thermal collector and flat plate bottom reflector with a gap between them, Energy Reports, ISSN 2352-4847, Elsevier, Amsterdam, Vol. 1, pp. 80-88, https://doi.org/10.1016/j.egyr.2014.10.004

This Version is available at:
https://hdl.handle.net/10419/187810

Energy Reports 1 (2015) 80–88

Contents lists available at ScienceDirect

Energy Reports

journal homepage: www.elsevier.com/locate/egyr

Theoretical analysis of solar thermal collector and flat plate bottom reflector with a gap between them

Hiroshi Tanaka *

Department of Mechanical Engineering, Kurume National College of Technology, Komorino, Kurume, Fukuoka 830-8555, Japan

ARTICLE INFO

Article history:
Received 1 September 2014
Received in revised form
8 October 2014
Accepted 17 October 2014
Available online 2 March 2015

ABSTRACT

Augmentation of solar radiation absorbed on a flat plate solar thermal collector by a flat plate bottom reflector was numerically determined when there was a gap between the collector and reflector. The inclination of both the collector and reflector was assumed to be adjustable according to the season. A mirror-symmetric plane of the collector to the reflector was introduced, and a graphical model was proposed to calculate the amount of solar radiation reflected by the reflector and then absorbed on the collector. The performance was analyzed for three typical days at a latitude of 30°N. Solar radiation absorbed on the collector can be increased by the bottom reflector even if there is a gap between the collector and reflector. The optimum inclinations of both the collector and reflector are almost the same while the gap length is less than the lengths of the collector and reflector. However, the range of inclination of the reflector that can increase the solar radiation absorbed on the collector decreases with an increase in gap length, and the solar radiation absorbed on the collector rapidly decreased with an increase in the gap length when the reflector and/or collector were not set at a proper angle.

1. Introduction

A booster reflector is an easy and inexpensive modification to add more solar energy to a solar thermal collector. Many studies have been performed to determine the optimum inclination angle of the top reflector (Rao et al., 1993; Hussein et al., 2000; Pucar and Despic, 2002), bottom reflector (McDaniels and Lowndes, 1975; Taha and Eldighidy, 1980; Arata and Geddes, 1986; Dang, 1986; Bollentin and Wilk, 1995; Hellstrom et al., 2003), and both the top and bottom reflectors (Chiam, 1982; Garg and Hrishikesan, 1988; Kostic et al., 2010a,b; Kostic and Pavlovic, 2012), where the top or bottom reflector extends from the upper or lower edge of the collector, respectively. Among them, Tanaka introduced graphical models to calculate the reflected radiation from the top (Tanaka, 2011a) or bottom (Tanaka, 2011b) reflector absorbed on the collector to determine the optimum inclination angle of both the collector and the top or the bottom reflector throughout the year at a 30°N latitude.

However, the collector–reflector systems that have been studied were only for cases in which the edges of the collector and reflector touched without a gap. Therefore, these models cannot be applied to the collector–reflector systems with a gap between the collector and reflector. However, there are many circumstances necessitating the installation of the booster reflector with a gap, especially to an already existing solar thermal collector, according to the limitations of the installation site.

Therefore, in this paper, the graphical model to calculate the solar radiation reflected from the bottom reflector and then absorbed on the collector when there is a gap between the collector and the bottom reflector is introduced. The analysis is performed for three typical days (spring equinox, summer solstice and winter solstice days) at 30°N latitude.

2. Theoretical analysis

2.1. Solar thermal collector and flat plate bottom reflector with a gap between them

A schematic diagram of the collector–reflector system with a gap analyzed in this paper is shown in Fig. 1. The solar thermal collector is assumed to be facing south, and the bottom reflector is placed on the southern side of the collector with a gap (l_g). The collector consists of a glass cover and absorbing plate. The bottom reflector is assumed to be made of a highly reflective material, such as a mirror-finished metal plate. The inclination angles of the collector and reflector from horizontal are θ_c and θ_m,

* Tel.: +81 942 35 9359; fax: + 81 942 35 9321.
E-mail address: tanakad@kurume-nct.ac.jp.

http://dx.doi.org/10.1016/j.egyr.2014.10.004

Nomenclature

G_{df}, G_{dr}	diffuse and direct solar radiation on a horizontal surface, W/m^2
l_c, l_m	length of collector and reflector, m
l_g	gap length between collector and reflector, m
$Q_{sun,re}$	absorption of reflected solar radiation, W/m^2
$Q_{sun,df}$, $Q_{sun,dr}$	absorption of diffuse and direct solar radiation, W/m^2
s_d	area of shadow of collector, m^2
s_r	area of overlapping part, m^2
w	width of collector and reflector, m
α_c	absorptance of absorbing plate
β	incident angle of sunrays to glass cover
β'	incident angle of reflected sunrays to glass cover
ϕ, φ	altitude and azimuth angle of the sun
θ_c, θ_m	angle of collector and reflector from horizontal
ρ_m	reflectance of reflector
τ_g	transmittance of glass cover
$(\tau_g)_{df}$	transmittance of glass cover for diffuse radiation

respectively, and the inclination angles of both the collector and reflector are assumed to be adjustable according to the season. Direct and diffuse solar radiation and also reflected radiation from the reflector transmit through the glass cover and are absorbed on the absorbing plate of the collector.

The design conditions and physical properties employed in this calculation are listed in Table 1. For simplification of the following calculations, the walls of the collector are disregarded, since the height of the walls (10 mm) is negligible in relation to the length (1 m) and width (1 m) of the collector.

Practically, solar radiation at lower levels cannot be utilized for the solar thermal collector due to heat loss. However, in this paper, it was assumed that solar radiation could be utilized even at lower levels.

2.2. Reflected radiation absorbed on the collector

The direct and reflected radiation concerning the collector–reflector system with a gap is shown in Fig. 2. The collector is shown as ABCD and the reflector is shown as EFGH. A distance between points A and E (or points B and F) is the gap length, l_g. The inclination angles of the collector and reflector from horizontal are θ_c and θ_m, and the length of the collector and the reflector is l_c and l_m, respectively. In this paper, the width of both the collector and reflector is determined to be the same as w. The altitude and azimuth angle of the sun is ϕ and φ, respectively. The direct radiation is shown as CC′, DD′, GG′ and HH′, and the reflected radiation is shown as GG″ and HH″. The reflected projection from the reflector casted on a horizontal surface is shown as EFG″H″. Not all of the reflected radiation could hit the collector, and a part of or all of the reflected radiation would escape to the ground without hitting the collector.

To calculate the amount of radiation reflected from the reflector and absorbed on the collector, a mirror-symmetric plane of the collector to the reflector is introduced and its side view is shown in Fig. 3. The amount of direct radiation that goes through the reflector and is then absorbed on the mirror-symmetric plane is exactly the same as that of the radiation that is reflected from the reflector and then absorbed on the collector. Here, from Fig. 3, the position of the top edge of the mirror-symmetric plane can be determined with length l_1 and l_2 as

$$l_1 = 2l_g \sin^2 \theta_m \tag{1}$$

$$l_2 = l_g \sin 2\theta_m. \tag{2}$$

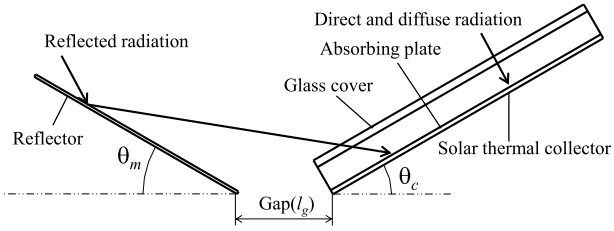

Fig. 1. Schematic diagram of collector–reflector system with a gap between the collector and reflector.

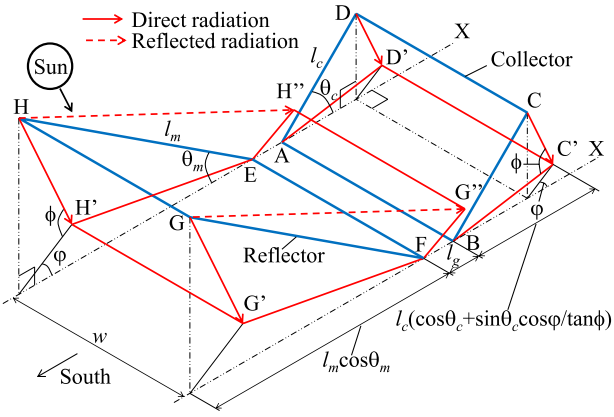

Fig. 2. Shadows of the collector (ABC′D′) and bottom reflector (EFG′H′) and reflected projection from the reflector (EFG″H″) on a horizontal surface caused by direct radiation.

Table 1
Design conditions and physical properties.

$w = 1$ m
$l_c = l_m = 1$ m
$\alpha_c = 0.9$, $\rho_m = 0.8$
$\tau_g(\beta)$ (Tanaka et al., 2000):
$\tau_g(\beta) = 2.642\cos\beta - 2.163\cos^2\beta - 0.320\cos^3\beta + 0.719\cos^4\beta$

The inclination angle of the mirror-symmetric plane from vertical is ω_1 and can be determined as

$$\omega_1 = 2\theta_m + \theta_c - \pi/2 \tag{3}$$

and Fig. 3 shows a case where angle ω_1 is positive ($\omega_1 > 0$). If ω_1 is negative ($\omega_1 < 0$), the length l_6 that is discussed below would be negative, but the following calculations are valid when l_6 has a negative value.

A schematic diagram to determine the amount of direct radiation that goes through the reflector and is then absorbed on the mirror-symmetric plane is shown in Fig. 4. The collector (ABCD) and reflector (EFGH) are exactly the same as those in Fig. 3, and the mirror-symmetric plane is shown as IJKL. The collector and reflector are placed on a horizontal surface (X), and the mirror-symmetric plane is placed on a virtual horizontal surface (X‴) that is $l_2 + l_3$ below from the horizontal surface (X). The shadows of the reflector and the mirror-symmetric plane caused by direct radiation on a virtual horizontal surface (X‴) are shown as E‴F‴G‴H‴ and I‴J‴KL, respectively. Therefore, the amount of direct radiation that goes through the reflector and is then absorbed on the mirror-symmetric plane, $Q_{sun,re}$, can be calculated by the area of the overlapping part of these shadows, s_r, in the form of a trapezoid I‴NG‴M as

$$Q_{sun,re} = G_{dr}\tau_g(\beta')\rho_m\alpha_c \times s_r \tag{4}$$

$$\cos\beta' = \sin\phi\cos\omega_1 + \cos\phi\sin\omega_1\cos\varphi \quad \text{(Japan Solar Energy Soc., 1985)} \tag{5}$$

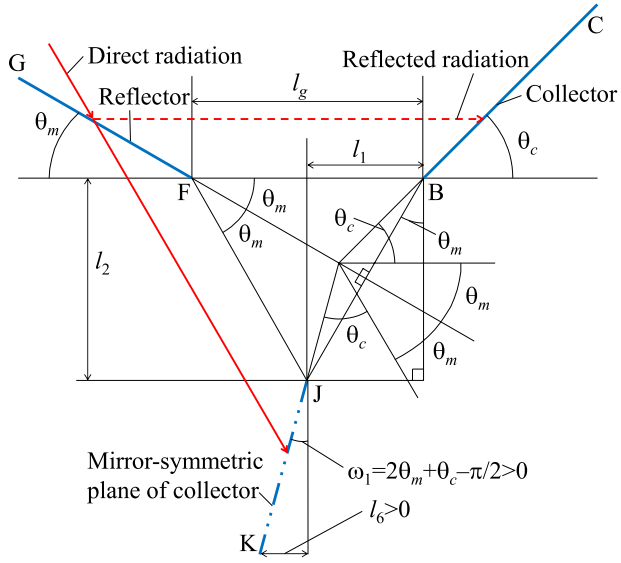

Fig. 3. Side view of mirror-symmetric plane of the collector to the reflector when ω_1 and l_6 are greater than zero.

where G_{dr} is the direct solar radiation on a horizontal surface, τ_g is the transmittance of the glass cover, β' is the incident angle of reflected sunrays to the glass cover, ρ_m is the reflectance of the reflector and α_c is the absorptance of the absorbing plate of the collector.

To determine the area of the overlapping part, s_r, lengths l_3 to l_{12} and angles ω_2 and ω_3 shown in Fig. 4 are determined as follows:

$$l_3 = l_c \cos\omega_1 \tag{6}$$

$$l_4 = l_c \sin\omega_1 \tag{7}$$

$$l_5 = l_3 \cos\varphi/\tan\phi \tag{8}$$

$$l_6 = l_3 \sin|\varphi|/\tan\phi \tag{9}$$

$$l_7 = l_m(\cos\theta_m - \sin\theta_m \cos\varphi/\tan\phi) \tag{10}$$

$$l_8 = l_m \sin\theta_m \sin|\varphi|/\tan\phi \tag{11}$$

$$l_9 = (l_m \sin\theta_m + l_2 + l_3)\cos\varphi/\tan\phi \tag{12}$$

$$l_{10} = l_m \cos\theta_m + l_g - l_1 - l_4 \tag{13}$$

$$l_{11} = l_9 + l_7 - l_{10} \tag{14}$$

$$l_{12} = (l_2 + l_3)\sin|\varphi|/\tan\phi \tag{15}$$

$$\tan\omega_2 = l_6/(l_4 + l_5) \tag{16}$$

$$\tan\omega_3 = l_8/l_7. \tag{17}$$

To calculate the area of the overlapping part, s_r, the four following cases should be considered.

Case 1 ($l_9 < l_{10}$ and $l_{12} + l_{11}\tan\omega_3 > w$)

When the shadow of the mirror-symmetric plane (I‴J‴KL) is behind that of the reflector (E‴F‴G‴H‴) (i.e. $l_9 < l_{10}$) and the shadow of the reflector does not pass through the line between points L and K (i.e. $l_{12} + l_{11}\tan\omega_3 > w$), the area of the overlapping part can be determined with the help of Fig. 5(a) as Case 1. If the shadow of the reflector does not exceed that of the mirror-symmetric plane (i.e. $l_9 + l_7 < l_{10} + l_4 + l_5$) shown as (i), the shadow of the reflector would be E‴(i)F‴(i)G‴H‴ and the overlapping part would be in the shape of a triangle OPF‴ (i). If the shadow of the reflector exceeds that of the mirror-symmetric plane (i.e. $l_9 + l_7 > l_{10} + l_4 + l_5$) shown as (ii), the overlapping part would be in the shape of a triangle OI‴Q. Therefore, the area of the overlapping part, s_r, for Case 1 can be determined as follows:

$$\text{(i) } l_9 + l_7 < l_{10} + l_4 + l_5\text{:}\quad s_r = 0.5 \times l_{15} \times l_{16} \tag{18}$$

$$\text{(ii) } l_9 + l_7 > l_{10} + l_4 + l_5\text{:}\quad s_r = 0.5 \times (l_4 + l_5 - l_{14}) \times l_{19} \tag{19}$$

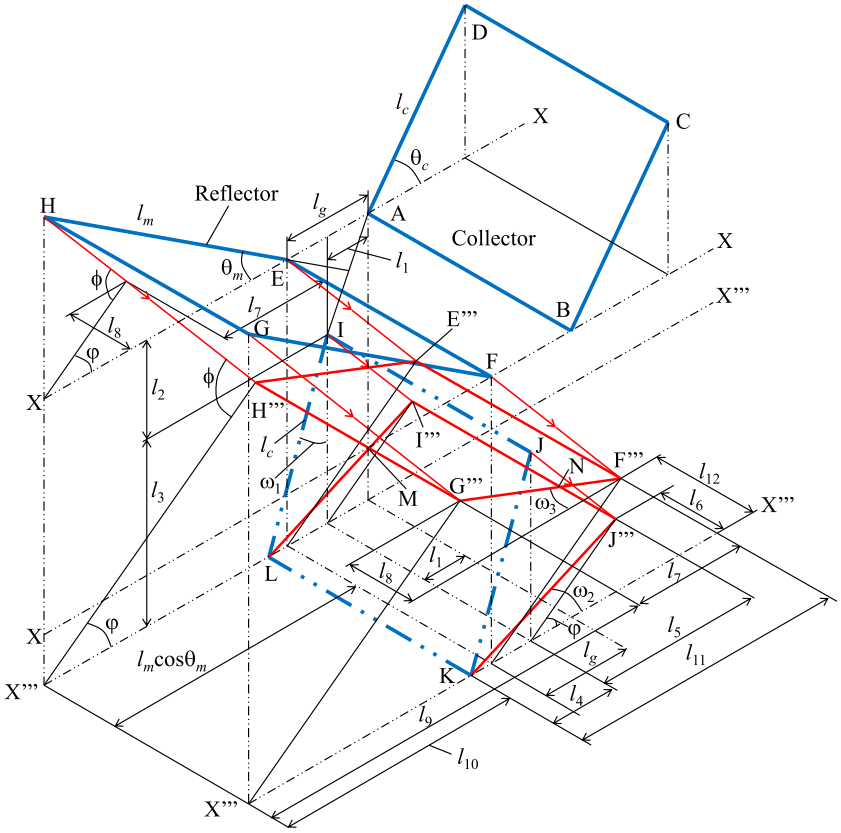

Fig. 4. Shadows of the reflector and the mirror-symmetric plane on a virtual horizontal surface X‴ caused by direct radiation to calculate the reflected radiation absorbed on the collector.

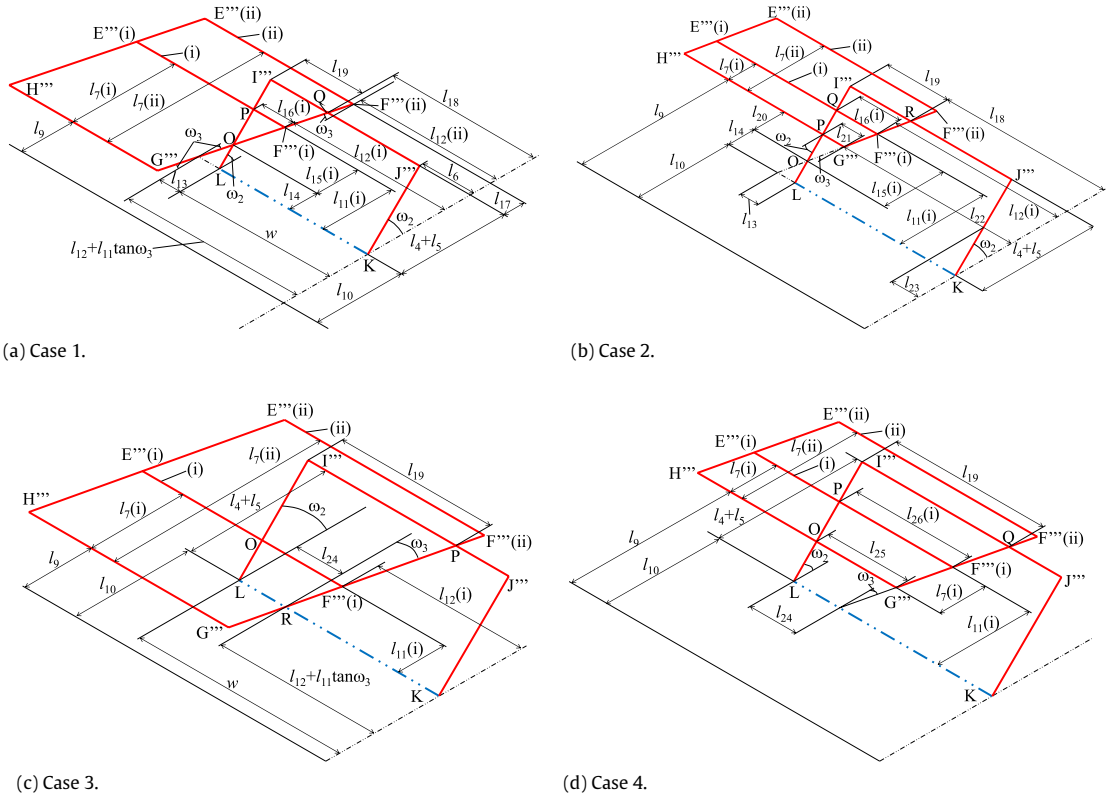

(a) Case 1. (b) Case 2.

(c) Case 3. (d) Case 4.

Fig. 5. The shadows of the reflector and the mirror-symmetric plane on a virtual horizontal surface X‴ ((a) for Case 1, (b) for Case 2, (c) for Case 3 and (d) for Case 4).

where

$$l_{13} = l_{12} + l_{11}\tan\omega_3 - w \tag{20}$$
$$l_{14} = l_{13}/(\tan\omega_2 + \tan\omega_3) \tag{21}$$
$$l_{15} = l_{11} - l_{14} \tag{22}$$
$$l_{16} = l_{15}(\tan\omega_2 + \tan\omega_3) \tag{23}$$
$$l_{17} = l_9 + l_7 - (l_{10} + l_4 + l_5) \tag{24}$$
$$l_{18} = l_{12} + l_{17}\tan\omega_3 \tag{25}$$
$$l_{19} = l_6 + w - l_{18}. \tag{26}$$

Case 2 ($l_9 > l_{10}$ and $l_{12} + l_{11}\tan\omega_3 > w$)

When the shadow of the reflector is behind that of the mirror-symmetric plane (i.e. $l_9 > l_{10}$) and $l_{12} + l_{11}\tan\omega_3 > w$, the area of the overlapping part can be determined with Fig. 5(b) as Case 2. If $l_9 + l_7 < l_{10} + l_4 + l_5$ shown as (i), the overlapping part would be in the shape of a trapezoid QF‴ (i) G‴P. If $l_9 + l_7 > l_{10} + l_4 + l_5$ shown as (ii), one would be in the shape of a trapezoid I‴RG‴P. Therefore, the area of the overlapping part for Case 2 can be determined as

$$\text{(i) } l_9 + l_7 < l_{10} + l_4 + l_5\text{:}\quad s_r = 0.5 \times l_7 \times (l_{16} + l_{21}) \tag{27}$$
$$\text{(ii) } l_9 + l_7 > l_{10} + l_4 + l_5\text{:}$$
$$s_r = 0.5 \times (l_{10} + l_4 + l_5 - l_9) \times (l_{19} + l_{21}) \tag{28}$$

where

$$l_{20} = l_9 - l_{10} - l_{14} \tag{29}$$
$$l_{21} = l_{20}(\tan\omega_2 + \tan\omega_3). \tag{30}$$

In Case 2, if $l_{22} > w + l_{23}$, the overlapping part would be in the shape of a triangle and the area s_r should be calculated with Eq. (18) and (19) for (i) and (ii), where

$$l_{22} = (l_m \sin\theta_m + l_2 + l_3)\sin|\varphi| \,/\, \tan\phi \tag{31}$$
$$l_{23} = (l_9 - l_{10})\tan\omega_2. \tag{32}$$

Case 3 ($l_9 < l_{10}$ and $l_{12} + l_{11}\tan\omega_3 < w$)

When the shadow of the reflector passes through the line between points L and K (i.e. $l_{12} + l_{11}\tan\omega_3 < w$) and $l_9 < l_{10}$, the area of the overlapping part can be determined in a similar manner as previous cases with the help of Fig. 5(c).

$$\text{(i) } l_9 + l_7 < l_{10} + l_4 + l_5 \text{ (a trapezoid OF‴(i)RL):}$$
$$s_r = 0.5 \times l_{11} \times \{2 \times l_{24} + l_{11}(\tan\omega_2 + \tan\omega_3)\} \tag{33}$$
$$\text{(ii) } l_9 + l_7 > l_{10} + l_4 + l_5 \text{ (a trapezoid I‴PRL):}$$
$$s_r = 0.5 \times (l_4 + l_5) \times (l_{19} + l_{24}) \tag{34}$$

where

$$l_{24} = w - (l_{12} + l_{11}\tan\omega_3). \tag{35}$$

Case 4 ($l_9 > l_{10}$ and $l_{12} + l_{11}\tan\omega_3 < w$)

When $l_9 > l_{10}$ and $l_{12} + l_{11}\tan\omega_3 < w$, the area of the overlapping part can be determined with the help of Fig. 5(d) as

$$\text{(i) } l_9 + l_7 < l_{10} + l_4 + l_5 \text{ (a trapezoid PF‴(i)G‴O):}$$
$$s_r = 0.5 \times l_7 \times \{l_{25} + l_{26}\} \tag{36}$$
$$\text{(ii) } l_9 + l_7 > l_{10} + l_4 + l_5 \text{ (a trapezoid I‴QG‴O):}$$
$$s_r = 0.5 \times (l_{10} + l_4 + l_5 - l_9) \times (l_{19} + l_{25}) \tag{37}$$

where

$$l_{25} = l_{24} + (l_9 - l_{10})(\tan\omega_2 + \tan\omega_3) \tag{38}$$
$$l_{26} = l_{24} + l_{11}(\tan\omega_2 + \tan\omega_3). \tag{39}$$

When the area of the overlapping part is calculated, there are some exceptions as follows:

1. Under the conditions below, the shadows never overlap and s_r equals zero.

(a) $l_9 + l_7 < l_{10} + l_{14}$ in Case 1(i) in Fig. 5(a) and $l_9 + l_7 < l_{10}$ in Case 3(i) in Fig. 5(c).

(b) $l_9 > l_{10} + l_4 + l_5$ in Cases 2 in Fig. 5(b) and Case 4 in Fig. 5(d).
(c) $l_{12} > w + l_{11} \tan\omega_2$ or $l_{18} > w + l_6$ in Cases 1 and 2.

2. When the sun moves north, that is, the absolute value of the azimuth angle of the sun, $|\varphi|$, is greater than 90°, in early morning and late evening during April to August, s_r should be calculated by making length l_5 negative.

2.3. Direct and diffuse radiation absorbed on the collector

The direct radiation absorbed on the collector, $Q_{sun,dr}$, can be determined as

$$Q_{sun,dr} = G_{dr}\tau(\beta)\alpha_c \times s_d \tag{40}$$

$$s_d = w l_c(\cos\theta_c + \sin\theta_c \cos\varphi/\tan\phi) \tag{41}$$

$$\cos\beta = \sin\phi\cos\theta_c + \cos\phi\sin\theta_c\cos\varphi \tag{42}$$

where β is the incident angle of sunrays to the glass cover. The term $w l_c(\cos\theta_c + \sin\theta_c\cos\varphi/\tan\phi)$ shows the shadow area of the collector caused by direct radiation shown as ABC′D′ in Fig. 2.

When the sun moves north in the early morning and in the late evening during the months of April to August, s_d in Eq. (40) would be

$$s_d = w l_c(\cos\theta_c - \sin\theta_c\cos\varphi/\tan\phi). \tag{43}$$

Diffuse solar radiation absorbed on the collector, $Q_{sun,df}$, can be determined assuming that diffuse radiation uniformly comes from all directions in the sky dome as

$$Q_{sun,df} = G_{df}(\tau_g)_{df}\alpha_c \times w l_c \tag{44}$$

where G_{df} is the diffuse solar radiation on a horizontal surface, and $(\tau_g)_{df}$ is a function of the inclination of the collector θ_c and is calculated by integrating the transmittance of the glass cover for diffuse radiation from all directions in the sky dome. This can be expressed as (Tanaka, 2011a)

$$(\tau_g)_{df} = -2.03 \times 10^{-5} \times \theta_c^2 - 2.05 \times 10^{-3} \times \theta_c + 0.667, \quad \theta_c[^\circ]. \tag{45}$$

Direct and diffuse solar radiation on a horizontal surface, G_{dr} and G_{df}, were calculated with Bouguer's equation and Berlage's equation respectively (Japan Solar Energy Soc., 1985), and mentioned in detail in a previous paper (Tanaka, 2011c).

2.4. Effect of the shadow of the reflector on the collector

When the altitude angle of the sun ϕ is small and/or the inclination angle of the bottom reflector is large, the reflector would shade a part of the collector. In this calculation, the effect of the shadow is taken into consideration. The shadow of the reflector on a horizontal surface is shown as EFG′H′ in Fig. 6(a). When the length l_{27} is longer than $l_m\cos\theta_m + l_g$ ($l_{27} > l_m\cos\theta_m + l_g$), the reflector shades the collector. If $l_{27} < l_m\cos\theta_m + l_g + l_c\cos\theta_c + l_{28}$, the shadow on the collector would be in the shape of a trapezoid NBOH′, and s_d in Eq. (40) would be

$$s_d = w l_c(\cos\theta_c + l_{28}) - l_{30}\{w - 0.5(l_{31} + l_8 - l_{32})\}. \tag{46}$$

Here, lengths l_{27} to l_{32} and angles ω_4 and ω_5 in Fig. 6(a) can be determined as follows:

$$l_{27} = l_m \sin\theta_m \cos\varphi/\tan\phi \tag{47}$$

$$l_{28} = l_c \sin\theta_c \cos\varphi/\tan\phi \tag{48}$$

$$l_{29} = l_c \sin\theta_c \sin|\varphi|/\tan\phi \tag{49}$$

$$l_{30} = l_{27} - (l_g + l_m\cos\theta_m) \tag{50}$$

$$l_{31} = l_g \tan\omega_4 \tag{51}$$

$$l_{32} = l_{30}\tan\omega_5 \tag{52}$$

$$\tan\omega_4 = l_8/(l_g + l_{30}) \tag{53}$$

$$\tan\omega_5 = l_{29}/(l_c\cos\theta_c + l_{28}). \tag{54}$$

If $l_{27} > l_m\cos\theta_m + l_g + l_c\cos\theta_c + l_{28}$ as shown in Fig. 6(b), the shaded area would be in the shape of a trapezoid PBC′N, and the amount of direct radiation absorbed on the collector would be the area APND′. Therefore, s_d in Eq. (40) would be

$$s_d = 0.5 \times (l_c\cos\theta_c + l_{28}) \times (l_{31} + l_{33}) \tag{55}$$

where

$$l_{33} = (l_g + l_c\cos\theta_c + l_{28})\tan\omega_4 - l_{29}. \tag{56}$$

As shown in Fig. 6(c), if $l_8 - w > l_{32}$ when $l_{30} < l_c\cos\theta_c + l_{28}$ (shown as (i)) or $\omega_4 > \omega_6$ when $l_{30} > l_c\cos\theta_c + l_{28}$ (shown as (ii)), the shaded area would be in the shape of a triangle PBN. Therefore, s_d in Eq. (40) would be

$$s_d = w(l_c\cos\theta_c + l_{28}) - 0.5(w - l_{31})^2/(\tan\omega_4 - \tan\omega_5) \tag{57}$$

where

$$\tan\omega_6 = (w + l_{29})/(l_g + l_c\cos\theta_c + l_{28}). \tag{58}$$

3. Results and discussion

Fig. 7 shows the theoretical predictions of the hourly variations of (a) the global solar radiation on a horizontal surface (Global) and the solar radiation absorbed on the collector with bottom reflector (RC) and one without a reflector (NC), and (b) the absorption of direct ($Q_{sun,dr}$), diffuse ($Q_{sun,df}$) and reflected ($Q_{sun,re}$) solar radiation on the collector on the spring equinox with varying the gap length l_g. The daily global solar radiation on a horizontal surface on this day is about 23.3 MJ/m^2 day. Here, the inclination angle of the collector θ_c was set to 35° and the reflector inclination θ_m was set to 30° and 40°, since the optimum inclination of the collector and the reflector was reported as $\theta_c = 35^\circ$ and $\theta_m = 30^\circ$ on the spring equinox day at 30°N when there is no gap between the collector and the reflector (Tanaka, 2011b). The solar radiation absorbed on the collector for RC was greater than that for NC, especially around noon. When $\theta_m = 30^\circ$, the hourly range through which the bottom reflector could reflect the sunrays to the collector as well as the amount of $Q_{sun,re}$ decreased with an increase in gap length l_g. However, $Q_{sun,re}$ at noon was almost the same for $l_g = 0$, 0.5 and 1 m. The reason is as follows. The altitude angle of the sun at noon on this day is about 60°, and the reflected radiation from the reflector with an inclination of 30° goes nearly horizontal. Therefore, the effect of gap length l_g on the amount of $Q_{sun,re}$ at noon was very little or negligible. However, if the reflector inclination was not at an optimum (e.g. $\theta_m = 40^\circ$), the amount of $Q_{sun,re}$ rapidly decreased with an increase in gap length l_g, and $Q_{sun,re}$ would be zero throughout the day at $l_g = 1$ m. This indicates that setting the reflector to the optimum inclination would be more important when there is a gap between the collector and reflector.

Isometric diagrams of (a) the daily solar radiation absorbed on the collector (MJ/m^2 day) as well as (b) changes in the daily absorbed radiation to a collector without reflector (θ_c is fixed at 30°) with varying inclinations of both collector θ_c and reflector θ_m for $l_g = 0$, 0.5 and 1 m on the spring equinox day, and summer and winter solstice days are shown in Fig. 8. Here, the daily global solar radiation on a horizontal surface on the summer and winter solstice days was about 30.3 and 12.6 MJ/m^2 day, respectively. The daily solar radiation absorbed on the collector was calculated at 1° intervals for both inclinations θ_c and θ_m on each day and for each gap length l_g. The optimum combination of inclinations θ_c and θ_m, which maximizes the daily solar radiation, varied considerably according to the season and was slightly affected by gap length l_g. The optimum inclination of collector θ_c was higher in the winter and lower in the summer and the optimum inclination of reflector θ_m was lower in the winter and higher in the summer at each gap

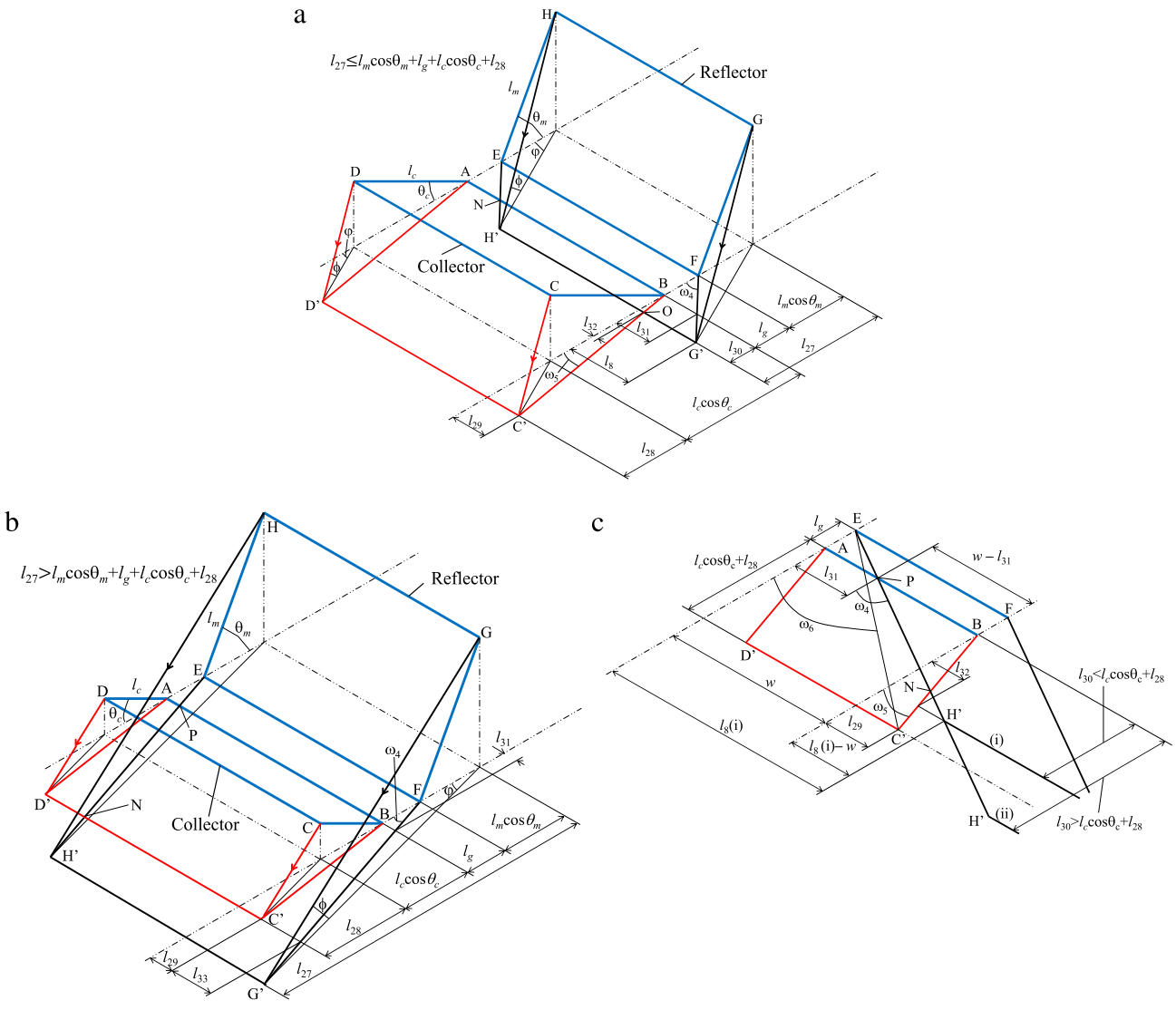

Fig. 6. The shadow of the reflector on the collector ((a) $l_{27} < l_m\cos\theta_m + l_g + l_c\cos\theta_c + l_{28}$, (b) $l_{27} < l_m\cos\theta_m + l_g + l_c\cos\theta_c + l_{28}$ and (c) the shadow would be in the shape of a triangle PBN).

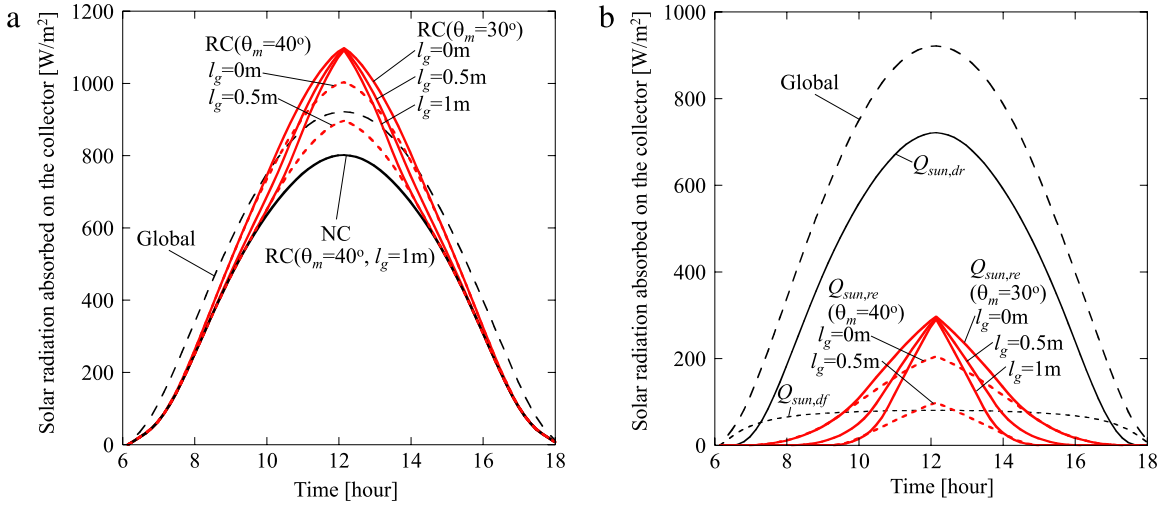

Fig. 7. Hourly variations of (a) solar radiation absorbed on the collector and (b) absorption of direct ($Q_{sun,dr}$), diffuse ($Q_{sun,df}$) and reflected ($Q_{sun,re}$) radiation on the collector with varying gap length l_g at reflector inclination $\theta_m = 30°$ and 40° when $\theta_c = 35°$ on a spring equinox day.

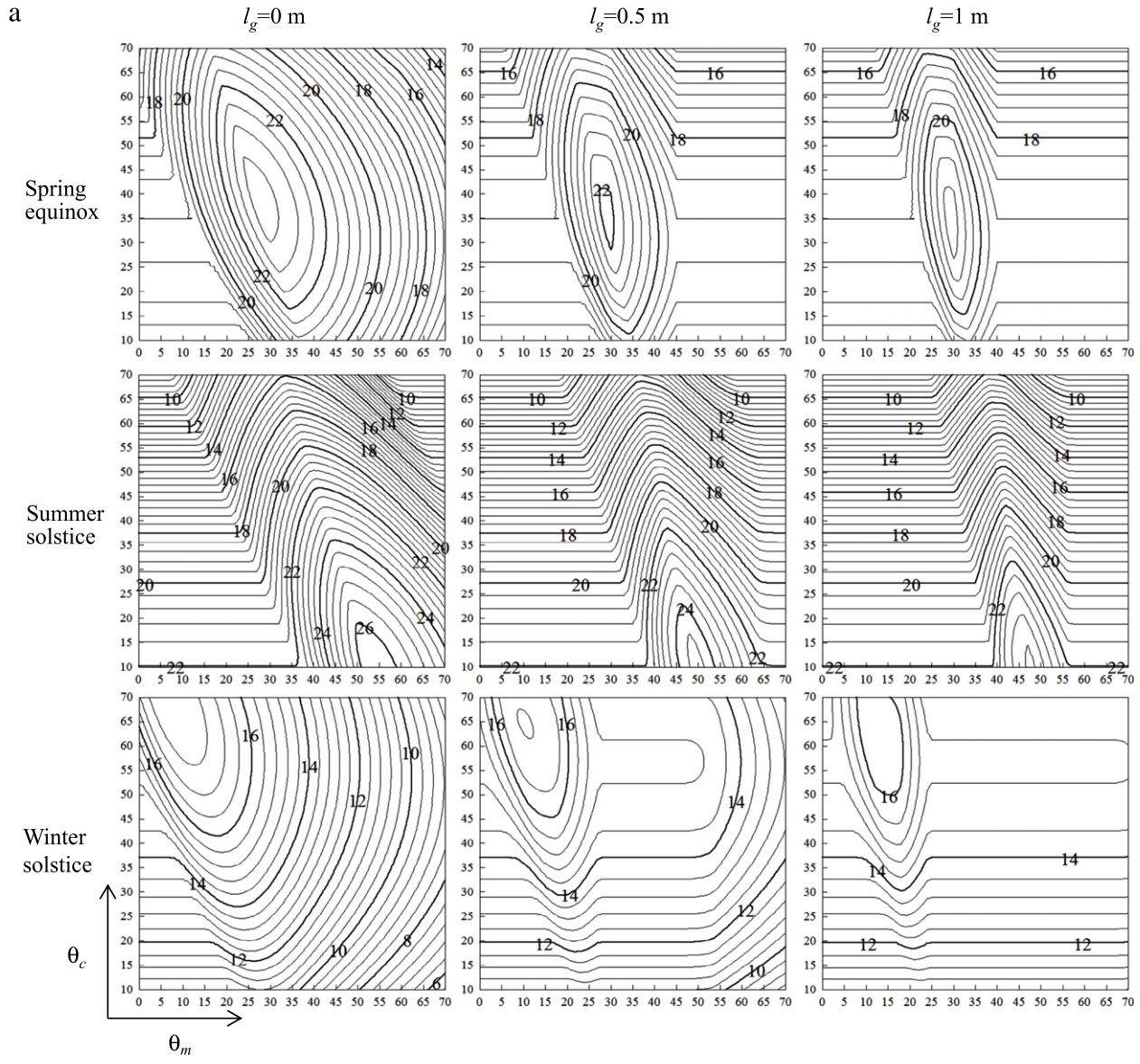

Fig. 8. Isometric diagrams of (a) daily solar radiation absorbed on the collector [MJ/m^2 day] and (b) changes in the daily absorbed radiation to a collector without reflector (θ_c is fixed at 30°) with varying inclinations θ_m and θ_c at l_g = 0, 0.5 and 1 m for three typical days.

length l_g, since the altitude angle of the sun is lower in the winter and higher in the summer.

If the optimum inclinations θ_c and θ_m are assumed to be set at 5° intervals to facilitate ease of adjustment, they should be fixed at $\theta_c = 35°$ and $\theta_m = 30°$ on the spring equinox and $\theta_c = 65°$ and $\theta_m = 10°$ on the winter solstice, and $\theta_c = 10°$ and $\theta_m = 45°$–$55°$ on the summer solstice depending on the gap length l_g, when the gap length l_g is in the range of 0–1 m.

The range of the reflector inclination that can increase the daily solar radiation decreases with an increase in gap length l_g, and would be about ±15° for $l_g = 0.5$ m and ±10° for $l_g = 1$ m from the optimum reflector inclination. Therefore, the reflector inclination should be carefully adjusted to the optimum inclination when the gap length is large.

On the spring equinox and the winter solstice days, a considerable decrease in daily solar radiation caused by the shadow of the reflector was observed when the reflector inclination θ_m was large at $l_g = 0$ m. However, the effect of the shadow of the reflector rapidly decreased with an increase in l_g, since the shadow of the reflector did not reach the collector at a larger gap length.

The daily solar radiation absorbed on the collector with varying reflector inclination θ_m is shown in Fig. 9. The results with an optimum collector inclination (35° in the spring, 10° in the summer and 65° in the winter) are shown in Fig. 9(a) and those with a fixed collector inclination of 30° (optimum collector inclination of a conventional flat plate solar thermal collector at 30°N) are shown in Fig. 9(b). The daily solar radiation can be increased both when the collector angle is optimally adjusted and when it is fixed at 30°, but the peak value of the daily solar radiation and the range of the reflector inclination that can increase the daily solar radiation decreased with an increase in gap length l_g. It should be noted that the reflector inclination θ_m should be determined in consideration of the collector inclination θ_c and/or gap length l_g, since the optimum reflector inclination varies with θ_c and l_g, especially in the summer.

The daily solar radiation absorbed on the collector with varying gap length l_g is shown in Fig. 10. Here, both the collector and reflector inclinations are determined as optimal with 5° intervals. Those inclinations were fixed at $\theta_c = 35°$ and $\theta_m = 30°$ on the spring equinox, $\theta_c = 65°$ and $\theta_m = 10°$ on the winter solstice

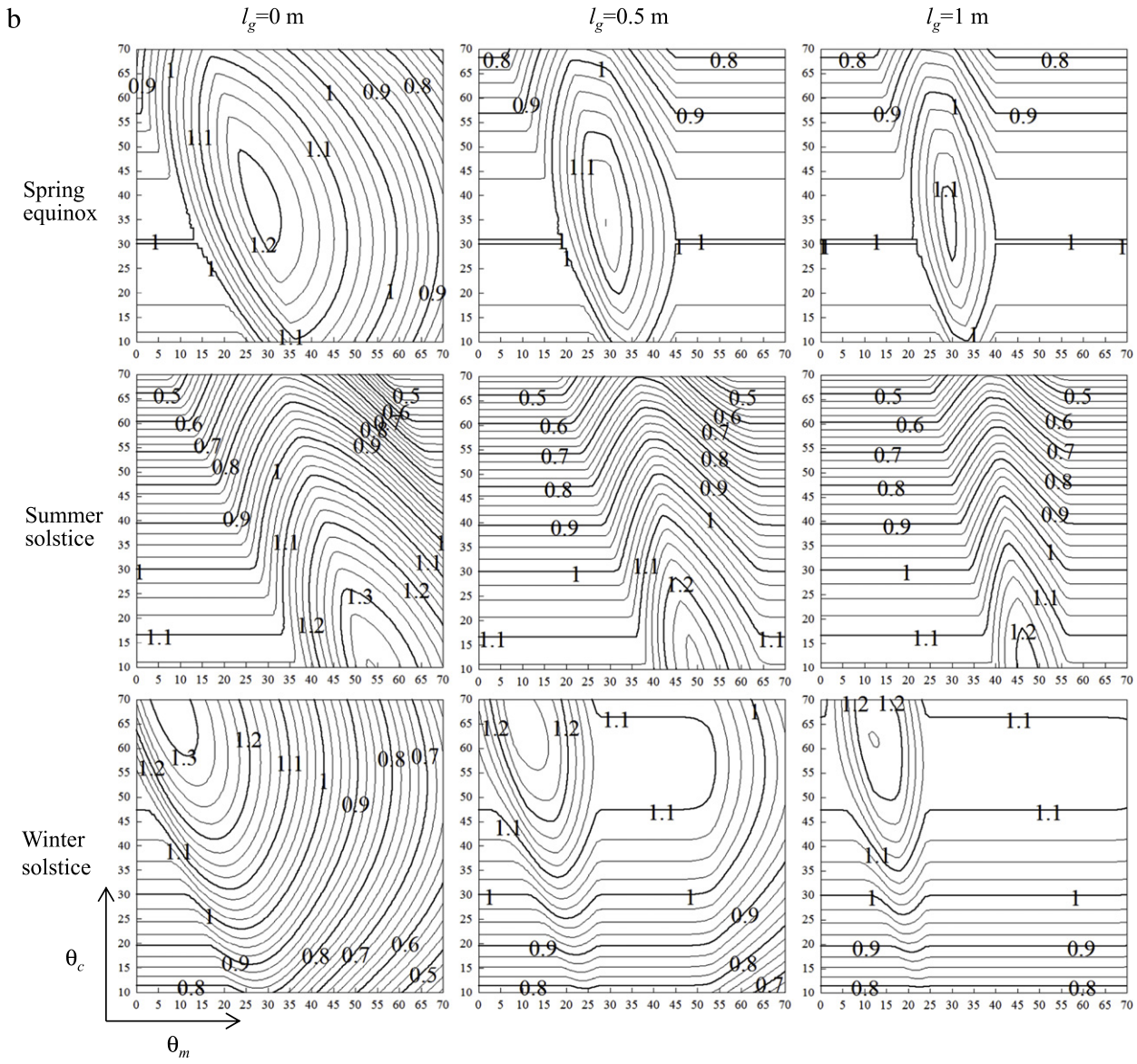

Fig. 8. (*continued*)

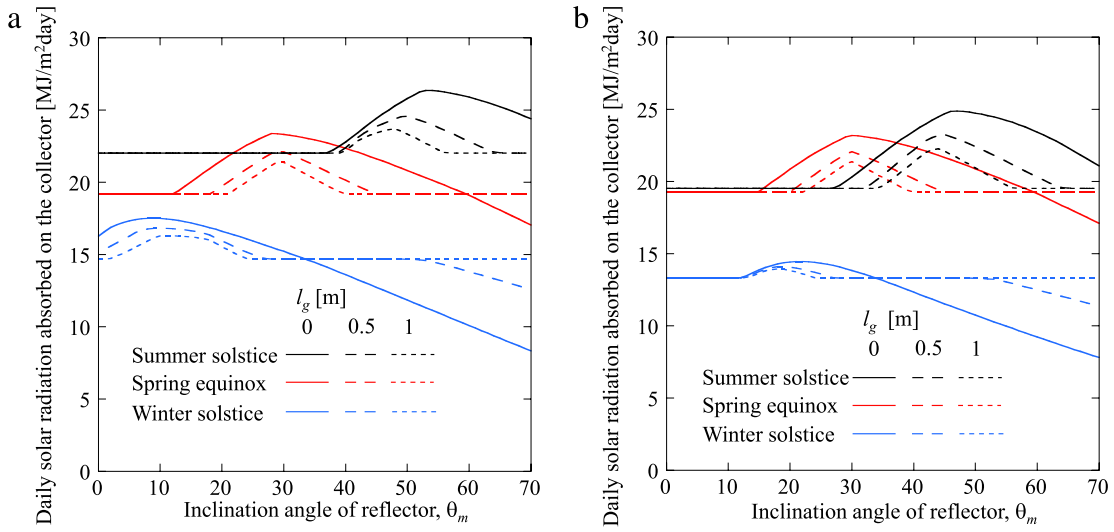

Fig. 9. The daily solar radiation absorbed on the collector with varying reflector inclination θ_m (a) with an optimum collector inclination and (b) with a fixed collector inclination ($\theta_c = 30°$) at $l_g = 0$, 0.5 and 1 m for three typical days.

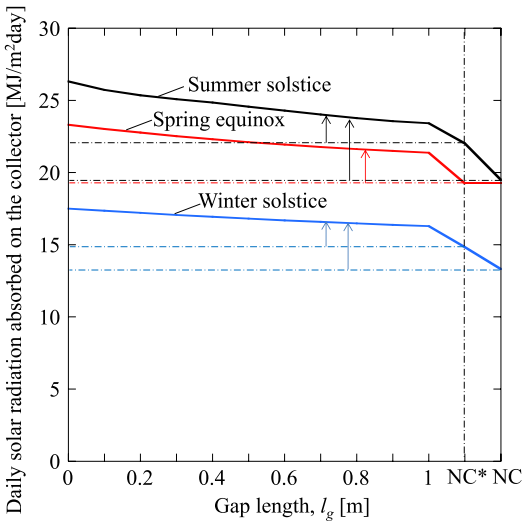

Fig. 10. The daily solar radiation absorbed on the collector with varying gap length l_g for three typical days.

for any gap length l_g, and θ_c was fixed at 10° and θ_m varied from 45° to 55° depending on the gap length l_g on the summer solstice. NC is the collector without a reflector with a fixed inclination of 30°, and NC* is a collector with an optimally-adjusted inclination (30° in the spring, 10° in the summer and 65° in the winter). The increase in the daily solar radiation gradually decreased with an increase in gap length l_g in all seasons. However, the daily solar radiation could be increased even if the gap length l_g was 1 m by adjusting the inclinations of the collector and reflector to the proper position. The increase in daily solar radiation by the bottom reflector when the gap length l_g was 0, 0.5 and 1 m was predicted to be 21%, 15% and 11% in the spring, 35%, 26% and 20% in the summer and 31%, 26% and 22% in the winter compared with NC (collector without reflector fixed at 30°), and 21%, 15% and 11% in the spring, 19%, 12% and 6% in the summer and 18%, 13% and 10% in the winter compared with NC* (collector without reflector with an optimal inclination). Therefore, it was found that the flat plate bottom reflector could work adequately even if there was a gap between the collector and reflector by setting the collector and/or the reflector to the proper position.

4. Conclusions

A flat plate solar thermal collector and a flat plate bottom reflector with a gap between the collector and reflector were theoretically analyzed using a graphical model for three typical days (on the spring equinox and summer and winter solstice days) at a latitude of 30°N. The effect of the reflector's shadow on the collector was also taken into account. The results of this work are summarized as follows:

(1) Solar radiation absorbed on the collector can be increased by the bottom reflector even if there is a gap between the collector and reflector.

(2) The optimum inclinations of both the collector and the reflector are almost the same while the gap length is less than the lengths of the collector and the reflector on the spring equinox and winter solstice days.

(3) With varying gap length, the optimum inclination of the collector is almost the same in each season but the optimum inclination of the reflector slightly varied.

(4) Solar radiation absorbed on the collector and the range of inclination of the reflector that can increase the solar radiation absorbed on the collector decrease with an increase in gap length.

(5) With an increase in gap length, solar radiation absorbed on the collector slightly decreases when both the inclinations of the collector and reflector were set to a proper angle, but the decrease was considerable when the inclinations of the collector and reflector were not set at an optimum position.

References

Arata, A.A., Geddes, R.W., 1986. Combined collector–reflector systems. Energy 11, 621–630.
Bollentin, J.W., Wilk, R.D., 1995. Modeling the solar irradiation on flat plate collectors augmented with planar reflectors. Sol. Energy 55, 343–354.
Chiam, H.F., 1982. Stationary reflector-augmented flat-plate collectors. Sol. Energy 29, 65–69.
Dang, A., 1986. Collector, Collector-reflector systems—an analytical and practical study. Energy Convers. Manage. 26, 33–39.
Garg, H.P., Hrishikesan, D.S., 1988. Enhancement of solar energy on flat-plate collector by plane booster mirrors. Sol. Energy 40, 295–307.
Hellstrom, B., Adsten, M., Nostell, P., Karlsson, B., Wackelgard, E., 2003. The impact of optical and thermal properties on the performance of flat plate solar collectors. Renew. Energy 28, 331–344.
Hussein, H.M.S., Ahmad, G.E., Mohamad, M.A., 2000. Optimization of operational and design parameters of plane reflector-tilted flat plate solar collector systems. Energy 25, 529–542.
Japan Solar Energy Soc., 1985. Solar Energy Utilization Handbook. Onkodo Press, Tokyo, p. 1, 7, 20.
Kostic, L.T., Pavlovic, Z.T., 2012. Optimal position of flat plate reflectors of solar thermal collector. Energy Build. 45, 161–168.
Kostic, L.T., Pavlovic, T.M., Pavlovic, Z.T., 2010a. Influence of reflectance from flat aluminum concentrators on energy efficiency of PV/thermal collector. Appl. Energy 87, 410–416.
Kostic, L.T., Pavlovic, T.M., Pavlovic, Z.T., 2010b. Optimal design of orientation of PV/T collector with reflectors. Appl. Energy 87, 3023–3029.
McDaniels, D.K., Lowndes, D.H., 1975. Enhanced solar energy collection using reflector-solar thermal collector combinations. Sol. Energy 17, 277–283.
Pucar, M.D.J., Despic, A.R., 2002. The enhancement of energy gain of solar collectors and photovoltaic panels by the reflection of solar beams. Energy 27, 205–223.
Rao, A.V.N., Chalam, R.V., Subramanyam, S., Rao, T.L.S., 1993. Energy contribution by booster mirrors. Energy Convers. Manage. 34, 309–326.
Taha, I.S., Eldighidy, S.M., 1980. Effect of off-south orientation on optimum conditions for maximum solar energy absorbed by flat plate collector augmented by plane reflector. Sol. Energy 25, 373–379.
Tanaka, H., 2011a. Solar thermal collector augmented by flat plate booster reflector: optimum inclination of collector and reflector. Appl. Energy 88, 1395–1404.
Tanaka, H., 2011b. Theoretical analysis of solar thermal collector with a flat plate bottom booster reflector. Energy Sci. Technol. 2 (2), 26–34.
Tanaka, H., 2011c. Tilted wick solar still with flat plate bottom reflector. Desalination 273, 405–413.
Tanaka, H., Nosoko, T., Nagata, T., 2000. A highly productive basin-type multiple-effect coupled solar still. Desalination 130, 279–293.